Published in final edited form as:
*Pediatr Res*. 2010 October ; 68(4): 275–280. doi:10.1203/PDR.0b013e3181ee0028.

# A Mouse Model of Conduction System Patterning Abnormalities in Heterotaxy Syndrome

**Richard J. Czosek**, **Allison Haaning**, and **Stephanie M. Ware**
Department of Pediatrics, Cincinnati Children's Hospital Medical Center, University of Cincinnati College of Medicine, Cincinnati, OH 45229

## Abstract

Duplication or absence of parts of the specialized cardiac conduction system in patients with heterotaxy syndrome causes significant clinical disease, but the mechanistic basis by which embryonic disruption of left-right patterning alters conduction system patterning in these patients is not well understood. We sought to determine whether a mouse model of X-linked human heterotaxy recapitulates conduction system abnormalities identified in heterotaxy patients. Cardiac structure and conduction system patterning were evaluated in Zic3 null embryos from e9.5 – 16.5 using genetic and molecular methods. Severe structural abnormalities involving atrial, ventricular and conotruncal development were associated with a spectrum of disorganized and ambiguous arrangements throughout the conduction system, including the appearance of duplicated structures. The severity and location of conduction system abnormalities correlated with the severity and location of associated structural heart disease and were identifiable at the earliest stages examined. The Zic3 mouse model provides a novel tool to dissect the mechanistic underpinnings of conduction system patterning and dysfunction and its relationship to cardiovascular malformations, making it a promising model to improve understanding and risk assessment in the clinical arena.

## INTRODUCTION

Heterotaxy syndrome is characterized by multiple congenital anomalies arising from defects in embryonic left-right patterning and loss of normal asymmetric laterality (1–3). The developing heart is particularly sensitive to left-right positional information, and abnormalties are associated with significant morbidity and mortality due to structural defects and/or arrhythmias (4). Heterotaxy patients are often described as being "bilateral left-sided" (left isomerism) or "bilateral right-sided" (right isomerism). Cardiac conduction system (CCS) abnormalities in the human heterotaxy population are thought to arise from either duplication or absence of one or more CCS elements resulting from similar left-right patterning abnormalities. Duplication creates a risk for tachycardias, while absence or dysfunction of sinoatrial (SA) or atrioventricular (AV) nodal elements can lead to brady-arrhythmias or heart block (5–7) and may require mechanical pacing (8). Heterotaxy syndrome itself is a risk factor for increased mortality (4).

In normal SA nodal development, the initial electrical pacemaker emerges at the inflow region of the linear heart tube (9) and develops adjacent to the venous sinus as it shifts rightward and is incorporated into the right atrium (10). As the SA node matures, there is increasing spatial restriction within the right atrium. The acute switch from ventricular activation emanating from the AV canal to a site at the ventricular apex at day mouse embryonic day 10.5–11.5 (e10.5–

Corresponding Author: Stephanie Ware M.D., Ph.D, Cincinnati Children's Hospital Medical Center, 240 Albert Sabin Way, MLC 7020, Cincinnati, OH 45229, Phone: (513) 636-9427, Fax: (513) 636-5958, Stephanie.ware@cchmc.org.

11.5) signals a primitive but functioning AV node and His-Purkinje system (11). Visualization of electrical system development in the mouse has been made possible through the use of several CCS transgenic mouse lines, including the CCS-*LacZ* and *minK-lacZ* models (11–15). Functional analysis has been achieved through the use of optical mapping using voltage-sensitive dye. In the CCS-*LacZ* model, this functional analysis has been correlated with anatomical staining patterns of CCS tissue elements (11). These tools have made possible the study of embryonic conduction system patterning; however, little is known about early embryonic patterning and development of the CCS in heterotaxy syndrome.

In humans, mutations of *ZIC3* cause the X-linked form of heterotaxy, the most common known genetic etiology of heterotaxy syndrome (2–3). ZIC3 is a zinc finger transcription factor and member of the GLI superfamily, important mediators of hedgehog signaling. Analysis of Zic3-null mice has demonstrated the importance of this gene in structural cardiac patterning (16–18). Although a comprehensive examination of cardiac development is lacking, the cardiac phenotypes identified mimic those seen in the human heterotaxy population (19).

In this study, we sought to describe CCS developmental patterning abnormalities in the Zic3 murine heterotaxy model using CCS-*LacZ* mice for anatomical visualization. Our results indicate that lack of Zic3 significantly affects normal CCS patterning and demonstrates a spatial correlation between structural and conduction system abnormalities. Importantly, the conduction system defects seen in this model are similar to those described in the human heterotaxy population. Ultimately, understanding CCS patterning, and its correlation with structural cardiac defects, may enhance our ability to develop new treatment strategies and provide risk counseling.

## METHODS

### Mouse embryo collection and β-Gal detection

Embryos were collected following timed matings. Zic3 null and control embryos were stage matched for analyses to within 0.5 days based on somite number (early embryos) or limb bud outgrowth and digit appearance (later embryos). CCS-*LacZ* embryos were stained with 5-bromo-4-chloro-3-indolyl-β-D-galactoside (X-Gal) staining solution as previously described (20). CCS-*LacZ* and Zic3 null/CCS-*LacZ* embryos were collected at e9.5 – e16.5 and fixed in 4% paraformaldehyde/PBS for 15 min at 4 °C and then rinsed in PBS. Embryos were stained with X-Gal solution at room temperature for 48 hours and post-fixed in 4% paraformaldehyde/PBS for 1 hr at 4 °C. This study was approved by the Cincinnati Children's Hospital Institutional Animal Care and Use Committee.

### Preparation of CCS-LacZ sections and photo imaging

Embryos were dehydrated through an increasing gradient of ethanol followed by multiple xylene washes and paraffin embedding. Sections were cut transversely at 12–14 μm using a microtome (Leica Microsystems, Wetzlar, German). Sections were deparaffinized in xylene, counterstained with eosin, dehydrated in xylene, and coverslipped using cytoseal (Electron Microscopy Sciences, Hatfield, PA). Images were captured using a Nikon DXM 1200F digital camera coupled to a Nikon Eclipse E400 microscope (Nikon Instruments Inc., Melville, NY).

### Synthesis of digoxigenin-labeled riboprobes

The cDNA sequence corresponding to amino acids 400–690 of *mHcn4* (base pairs 1198–2068 of NM_001081192) was amplified from mouse heart RNA with the primers 5′-ATATCTAGACAGTG GGAAGAGATCTTCCA-3′ and 5′-ATACTCGAGTGAAGTTGTCCACGCTCAGT–3′ and subcloned into the *Xba*I-*Xho*I sites of pBluescript II SK(-). This region of *mHcn4* effectively labels specific components of the

adult mouse central nervous system (21) and has been identified as a marker of the SA node. The *mNkx2–5* riboprobe plasmid was kindly provided by Dr. Yutzey (22). Antisense riboprobes were generated by in vitro transcription with the appropriate RNA polymerase in the presence of DIG RNA labeling mix.

### In situ hybridization

In situ hybridization was performed as previously described (23). Paraffin embedded embryos were sectioned transversely, and 12–14 μm sections were mounted on Superfrost Plus microscope slides (Thermo Fisher Scientific, Waltham, MA). Sections were hybridized with 200 μl of digoxigenin-labeled riboprobe at 1 μg/ml in incubation chambers (22 × 40 × 0.2 mm, Electron Microscopy Sciences, Hatfield, PA). Color development was performed using BM Purple (Roche Applied Science, Indianapolis, IN) for 8–12 hours.

## RESULTS

### Development of Structural Cardiac Abnormalities in Zic3 null mice

Patients with heterotaxy have a diverse spectrum of cardiovascular malformations (CVM). In order to evaluate the cardiac anomalies in a mouse model of heterotaxy, embryos were evaluated from e9.5 – e16.5. Structural cardiac abnormalities decreased at later embryonic stages (40% of nulls had structurally abnormal hearts at e10.5, 32% at e11.5, and 25% at e12.5) and a reduction in litter size after e10.5, consistent with embryonic lethality caused by complex congenital malformations. The cardiac phenotypes in Zic3 deficient embryos were variable, and recapitulated the spectrum of phenotypes seen in human heterotaxy syndrome. Gross examination of the hearts at e10.5 – e12.5 demonstrated a range of phenotypes including univentricular morphology and conotruncal abnormalities (Fig. 1 and data not shown). By e10.5, the heart has undergone d-looping of the ventricular chambers and the common outflow tract has looped as a precursor to development of normal great artery relationship. The developing atrial chambers lie posterior to two well developed ventricular chambers and the outflow tract arises from the right ventricle (Fig. 1A). Fig. 1B demonstrates d-looping with conotruncal malposition in a Zic3 null embryo, with the common outflow arising vertically and centrally from the most superior aspect of the ventricular chambers. The atria are abnormally positioned inferior to the ventricular chambers. Fig. 1C demonstrates l-looped malposition of the outflow tract and inferior displacement of the atria. While wild type embryos have two developing ventricles at e10.5, a subset of Zic3 null embryos demonstrate univentricular morphology (Fig. 1C-D), with a single ventricular chamber giving rise to a single outlet. Conotruncal abnormalities were common and always associated with additional structural abnormalities. The range of defects in cardiac looping observed during cardiac development in these null mice provides insight into the variable phenotypic presentations of patients with heterotaxy.

### Sinoatrial Nodal Development

CCS development in patients with heterotaxy syndrome has been associated with loss of the normal asymmetric restriction of the SA node within the right atrium. Both inversion of the SA node with a single pacemaker in the left atrium, as well as duplication or “twinning” of the SA node with both right and left atrial intrinsic pacemakers have been described. Genetic and molecular methods were used to investigate SA node development in Zic3 null mice. Mating Zic3 mice with CCS-*LacZ* mice allowed for visulaization of CCS development in Zic3 null embryos based on the staining pattern. Abnormalities in SA nodal development in Zic3 deficient embryos ranged from apparently normal to severely abnormal. There was strong correlation between the presence of structural defects and abnormal SA node patterning: Zic3 null embryos with normal structural anatomy had normal SA nodal staining patterns, while embryos with abnormal structure displayed either normal or abnormal SA nodal patterning.

Abnormalities in left-right patterning were identified based on loss of normal SA node lateralization and restriction within the right atrium (Fig. 2). These findings are similar to those found in clinical descriptions of SA nodal development in the human heterotaxy population. Normal SA node staining is restricted to the right atrium and right sinus valve (Fig. 2A-C) and the pattern of staining is somewhat diffuse at developmental stages younger than e10.5. As development continues, the staining pattern becomes progressively more restricted to the superior right atrium adjacent to the superior vena cava and the venous valve, the general location of the mature SA node. In Zic3 null embryos, two patterns of SA nodal development were seen. Examples of SA node inversus were found, both with SA nodal development restricted to the left atrium as well as bilateralization of SA node development. Failure of proper lateralization of the SA node indicates ambiguous patterning consistent with right atrial isomerism (Fig. 2D-F). Fig. 2G-I demonstrates a left-sided SA node in a null embryo with l-looping.

SA node development in Zic3 null embryos was evaluated further using molecular methods. Previous studies have elaborated a molecular pathway for localized formation of the SA node (24–26). The atrial myocardium is characterized by expression of myocardial markers such as *Nppa* and *Nkx2.5*, whereas the non-myocardial SA node region expresses markers such as the pacemaker channel gene product, *Hcn4*. During heart tube maturation, Nkx2.5 progressively represses expression of *Hcn4*, resulting in molecular delineation of a distinct, compact SA node region in the right atrium. To determine whether specification of the SA node occurs properly in Zic3 null embryos, the expression of *Nkx2.5* and *Hcn4* was determined by in situ hybridization. In e11.5 wild type embryos, the SA node is a triangular wedge of tissue which is *Hcn4* positive and *Nkx2.5* negative (Fig. 3A-C). At these stages, *Hcn4* expression is localized to the same anatomic structures identified by X-gal staining in CCS-*LacZ* mice, but is more spatially restricted in its expression profile. Zic3 null embryos (Fig. 3D-I) retain the mutually exclusive expression pattern of *Hcn4* and *Nkx2.5* identified in wild type embryos; however, the positioning and morphology of the SA node tissue is abnormal. There is a diffuse appearance to some SA nodal structures, as well as abnormal shape and positioning (Fig. 3E, F, H, I). The expression pattern in embryos with bilateral staining (Fig. 3G, bilateral SA nodes) tended to be more diffuse and heterogeneous compared to the wild type patterning. These results imply that Zic3 is not required for SA node specification but plays a central role in proper localization.

## Organization of CCS after Completion of Cardiac Looping

By e12.5, the final phases of cardiac looping are complete and restriction and maturation of CCS patterning occurs. In Zic3 null embryos, structural defects are present along with SA node morphogenesis and abnormal development of the distal conduction system (Fig. 4). SA node development at e12.5 is characterized by further restriction and organization of the staining pattern within the right atrium (Fig. 4). In contrast, SA node tissue in Zic3 null embryos at e12.5 demonstrates diffuse, disorganized X-gal staining patterns within the atrial chamber, in addition to the bilateralization of the staining (Fig 4F, J, K). These results provide evidence of failure to properly pattern the SA node. Additionally, the diffuse and disorganized appearance of SA node staining suggests a possible temporal disruption, with retention of primitive patterning features. Absence of SA nodal staining, suggestive of left atrial isomerism was also identified (data not shown).

Distal conduction system abnormalities, involving the AV node, His bundle or Purkinje system, in patients with heterotaxy can result in both abnormal positioning and duplication of CCS elements. “Twinning” or duplication of the AV node in humans may lead to a form of re-entry tachycardia. Distal conduction system patterning demonstrated a relationship between structural and CCS patterning defects similar to that observed in more proximal SA nodal

development. Again, Zic3 null embryos with normal cardiac structure demonstrated universally normal distal conduction system patterning. In hearts with structural abnormalities, the distal conduction system was abnormal to varying degrees in all embryos analyzed (Table 1). Prior to e10.5, the entire AV canal functions as AV nodal tissue and the staining pattern is circumferential, encompassing the entire periphery of the AV canal region. Following a timeline similar to SA node maturation, the AV node becomes restricted to its adult position and initiates compaction and organization by e12.5 (Fig. 4A-D). Distal to the AV node the compacted CCS continues as a linear band of tissue extending to the distal Purkinje system through the right posterior aspect of the AV canal and right ventricular region (Fig. 4D).

In abnormal Zic3 null embryos, patterning was disrupted at the level of the AV node, His bundle, and bundle branches. Abnormalities of the AV node included disorganization with loss of normal compaction characterized by diffuse staining (Fig 4G). Rarely, duplication of AV nodal tissue was visualized. His bundle and bundle branch patterning were also significantly affected. The staining around the periphery of the AV canal in Fig. 4I-L illustrates the failure to restrict CCS patterning distal to the AV node. The typical single linear band extending from the AV node to the distal Purkinje system is replaced by two tracts. Staining patterns consistent with accessory connections from the atrium and ventricle were also identified in a subset of embryos, possibly indicating future phenotypic accessory pathway development (Fig 4F, K). These findings indicate that deficiency of Zic3 can severely affect embryonic patterning of the distal conduction system and imply a strong relationship between abnormalities in cardiac structure and the distal conduction system. Importantly, these abnormalities are similar to those commonly seen in the human heterotaxy population (Table 2).

## DISCUSSION

In humans, heterotaxy syndrome is associated with severe cardiac structural and conduction system abnormalities and is an independent risk factor for post-operative mortality following surgical palliation (3,5). The clinical impact of these conduction system abnormalities has been based on postnatal functional assessment with bradycardia or heart block. Although the molecular cues important for development of conduction system lineage are beginning to be elaborated (24–26), the embryonic events controlling conduction system pattern formation are largely unknown. In this study, we examined conduction system development and its association with structural development in the Zic3 heterotaxy mouse model.

Loss of normal left-right differentiation affects CCS patterning. All structurally abnormal Zic3 null hearts exhibited CCS abnormalities. However, even at these early developmental stages, there were no embryos with completely identical cardiac abnormalities in our series, consistent with the clinical heterogeneity of heterotaxy. In the proximal CCS, SA node duplication was the most common finding (right isomerism, n=7/18 sectioned embryos). In addition, lack of SA nodal development (left isomerism, n=4/18) and exclusive left atrial staining associated with complete reversal of myocardial and CCS structures (situs inversus, n=3/18) were identified. These abnormalities of duplicated or absent CCS elements mimic those seen in the human heterotaxy population (27–29). Hypoplasia of the SA node has been associated with aberrant lineage specification, as manifest by ectopic expression of *Nkx2.5*, in mouse models such as Shox2 null mice (30). In contrast, Zic3 null mice form a normal boundary of *Hcn4* and *Nkx2.5* expression in the atria, indicating that Zic3 deficiency does not impair lineage specification or the molecular signature of the SA node and will therefore be a useful tool to dissect the secondary consequences of abnormal left-right patterning on SA node patterning, structural malformation and ultimately CCS function.

Clinically, left atrial isomerism leads to brady-arrhythmias secondary to SA node dysfunction, while right atrial isomerism is associated with sinus propagation alternating between the right

and left sided intrinsic pacemakers (8,29). Understanding how SA node patterning affects function is therefore clinically relevant. The current studies cannot rule out the possibility that Zic3 deficient mice with normal appearing staining patterns have inherent functional abnormalities. Future studies assessing functional characteristics via voltage gated visualization embryonically (11), or intracardiac electrophysiology testing postnatally could help resolve this question (31).

In addition to the SA nodal abnormalities described, Zic3 deficient embryos also demonstrate abnormal AV nodal patterning. Prior to e10.5, staining circumferentially around the AV canal appears normal in Zic3 null embryos. After e10.5, AV node abnormalities including disorganization, malpositioning, or mislocalization are identified (n=6/9 d12.5 sectioned embryos), similar to abnormalities seen in SA nodal patterning. This pattern is consistent with human pathology studies in which both AV nodal structures are displaced and can be dysfunctional (32). Similar inhibition of distal CCS compaction including alterations in AV node and His-purkinje system disorganization is seen upon neural crest ablation (33).

In Zic3 null embryos, there was evidence of additional AV pathways consistent with conventional accessory pathways or Mahaim connections (n =2/9), a common finding in patients with heterotaxy syndrome and L-looped ventricular configuration that can result in the typical form of AV reciprocating tachycardia (34). The CCS-*LacZ* model has been used previously to describe CCS abnormalities such as Mahaim fiber development and delineation of embryonic cardiac regions with future arrhythmogenic potential (13–14).

Zic3 null mice exhibit mixed morphologies (eg. right or left isomerism) indicating that they encompass the full range of hetertoaxy spectrum defects. Mouse models with exclusive right or left isomeric patterns, such as Pitx2 or Lefty-1 knockouts, have been described anatomically but have not been analyzed in depth with regard to CCS development (35–36). Clinically, understanding how conduction system patterning correlates with congenital heart disease is important for management.

In summary, proper patterning of the CCS requires a complex interplay of embryonic left-right differentiation. CCS abnormalities in the Zic3 heterotaxy model are closely linked with associated abnormalities of cardiac structure. Loss of Zic3 leads to abnormal CCS structure and maturation that coincides with the severity and location of associated structural heart disease. Potential mechanisms for this disruption include ambiguous patterning, duplication of tissue patterning and/or failure of progressive development with retention of earlier embryonic patterns. The congruent relationship of structural and CCS patterning abnormalities seem to indicate shared regulatory programs directing developmental patterning though future lineage studies will be needed to more clearly delineate this relationship. This mouse model provides a novel tool to dissect the genetic regulatory hierarchy linking left-right patterning with conduction system specific gene expression and pattern formation as well as elucidation of human rhythm abnormalities.

## Acknowledgments

We thank Glenn Fishman for the use of the CCS-*LacZ* reporter mouse line.

This study was funded by grant number RO1 HL088639 [to S.M.W.] from National Institutes of Health.

## ABBREVIATIONS

| | |
|---|---|
| AV | atrioventricular |
| CCS | Cardiac conduction system |

| | |
|---|---|
| CVM | cardiovascular malformations |
| SA | sinoatrial |

## References


1. Ramsdell AF. Left-right asymmetry and congenital cardiac defects: getting to the heart of the matter in vertebrate left-right axis determination. Dev Biol 2005;288:1–20. [PubMed: 16289136]
2. Sutherland MJ, Ware SM. Disorders of left-right asymmetry: heterotaxy and situs inversus. Am J Med Genet C Semin Med Genet 2009;151C:307–317. [PubMed: 19876930]
3. Belmont JW, Mohapatra B, Towbin JA, Ware SM. Molecular genetics of heterotaxy syndromes. Curr Opin Cardiol 2004;19:216–220. [PubMed: 15096953]
4. Jacobs JP, O'Brien SM, Chai PJ, Morell VO, Lindberg HL, Quintessenza JA. Management of 239 patients with hypoplastic left heart syndrome and related malformations from 1993 to 2007. Ann Thorac Surg 2008;85:1691–1696. discussion 1697. [PubMed: 18442568]
5. Wilkinson JL, Smith A, Lincoln C, Anderson RH. Conducting tissues in congenitally corrected transposition with situs inversus. Br Heart J 1978;40:41–48. [PubMed: 626661]
6. Cheung YF, Cheng VY, Yung TC, Chau AK. Cardiac rhythm and symptomatic arrhythmia in right atrial isomerism. Am Heart J 2002;144:159–164. [PubMed: 12094203]
7. Epstein MR, Saul JP, Weindling SN, Triedman JK, Walsh EP. Atrioventricular reciprocating tachycardia involving twin atrioventricular nodes in patients with complex congenital heart disease. J Cardiovasc Electrophysiol 2001;12:671–679. [PubMed: 11405401]
8. Wu MH, Wang JK, Lin JL, Lai LP, Lue HC, Hsieh FJ. Cardiac rhythm disturbances in patients with left atrial isomerism. Pacing Clin Electrophysiol 2001;24:1631–1638. [PubMed: 11816632]
9. Gourdie RG, Harris BS, Bond J, Justus C, Hewett KW, O'Brien TX, Thompson RP, Sedmera D. Development of the cardiac pacemaking and conduction system. Birth Defects Res C Embryo Today 2003;69:46–57. [PubMed: 12768657]
10. Moorman AF, de Jong F, Denyn MM, Lamers WH. Development of the cardiac conduction system. Circ Res 1998;82:629–644. [PubMed: 9546372]
11. Rentschler S, Vaidya DM, Tamaddon H, Degenhardt K, Sassoon D, Morley GE, Jalife J, Fishman GI. Visualization and functional characterization of the developing murine cardiac conduction system. Development 2001;128:1785–1792. [PubMed: 11311159]
12. Kondo RP, Anderson RH, Kupershmidt S, Roden DM, Evans SM. Development of the cardiac conduction system as delineated by minK-lacZ. J Cardiovasc Electrophysiol 2003;14:383–391. [PubMed: 12741710]
13. Jongbloed MR, Schalij MJ, Poelmann RE, Blom NA, Fekkes ML, Wang Z, Fishman GI, Gittenberger-De Groot AC. Embryonic conduction tissue: a spatial correlation with adult arrhythmogenic areas. J Cardiovasc Electrophysiol 2004;15:349–355. [PubMed: 15030427]
14. Jongbloed MR, Wijffels MC, Schalij MJ, Blom NA, Poelmann RE, van der Laarse A, Mentink MM, Wang Z, Fishman GI, Gittenberger-de Groot AC. Development of the right ventricular inflow tract and moderator band: a possible morphological and functional explanation for Mahaim tachycardia. Circ Res 2005;96:776–783. [PubMed: 15761198]
15. Myers DC, Fishman GI. Toward an understanding of the genetics of murine cardiac pacemaking and conduction system development. Anat Rec A Discov Mol Cell Evol Biol 2004;280:1018–1021. [PubMed: 15368345]
16. Purandare SM, Ware SM, Kwan KM, Gebbia M, Bassi MT, Deng JM, Vogel H, Behringer RR, Belmont JW, Casey B. A complex syndrome of left-right axis, central nervous system and axial skeleton defects in Zic3 mutant mice. Development 2002;129:2293–2302. [PubMed: 11959836]
17. Ware SM, Harutyunyan KG, Belmont JW. Heart defects in X-linked heterotaxy: evidence for a genetic interaction of Zic3 with the nodal signaling pathway. Dev Dyn 2006;235:1631–1637. [PubMed: 16496285]
18. Ware SM, Harutyunyan KG, Belmont JW. Zic3 is critical for early embryonic patterning during gastrulation. Dev Dyn 2006;235:776–785. [PubMed: 16397896]

19. Ware SM, Peng J, Zhu L, Fernbach S, Colicos S, Casey B, Towbin J, Belmont JW. Identification and functional analysis of ZIC3 mutations in heterotaxy and related congenital heart defects. Am J Hum Genet 2004;74:93–105. [PubMed: 14681828]
20. MacGregor, GR.; Nolan, GP.; Fiering, S.; Roederer, M.; Herzenberg, LA. Use of E. Coli lacZ (β-Galactosidase) as a reporter gene. In: Murray, EJ., editor. Gene Transfer and Expression Protocols. The Humana Press Inc; Clifton: 1991. p. 217-235.
21. Santoro B, Chen S, Luthi A, Pavlidis P, Shumyatsky GP, Tibbs GR, Siegelbaum SA. Molecular and functional heterogeneity of hyperpolarization-activated pacemaker channels in the mouse CNS. J Neurosci 2000;20:5264–5275. [PubMed: 10884310]
22. Searcy RD, Vincent EB, Liberatore CM, Yutzey KE. A GATA-dependent nkx-2.5 regulatory element activates early cardiac gene expression in transgenic mice. Development 1998;125:4461–4470. [PubMed: 9778505]
23. Shelton EL, Yutzey KE. Tbx20 Regulation of Endocardial Cushion Cell Proliferation and Extracellular Matrix Gene Expression. Dev Biol 2007;302:376–388. [PubMed: 17064679]
24. Hoogaars WM, Engel A, Brons JF, Verkerk AO, de Lange FJ, Wong LY, Bakker ML, Clout DE, Wakker V, Barnett P, Ravesloot JH, Moorman AF, Verheijck EE, Christoffels VM. Tbx3 controls the sinoatrial node gene program and imposes pacemaker function on the atria. Genes Dev 2007;21:1098–1112. [PubMed: 17473172]
25. Hoogaars WM, Tessari A, Moorman AF, de Boer PA, Hagoort J, Soufan AT, Campione M, Christoffels VM. The transcriptional repressor Tbx3 delineates the developing central conduction system of the heart. Cardiovasc Res 2004;62:489–499. [PubMed: 15158141]
26. Mommersteeg MT, Hoogaars WM, Prall OW, de Gier-de Vries C, Wiese C, Clout DE, Papaioannou VE, Brown NA, Harvey RP, Moorman AF, Christoffels VM. Molecular pathway for the localized formation of the sinoatrial node. Circ Res 2007;100:354–362. [PubMed: 17234970]
27. Dickinson DF, Wilkinson JL, Anderson KR, Smith A, Ho SY, Anderson RH. The cardiac conduction system in situs ambiguus. Circulation 1979;59:879–885. [PubMed: 428099]
28. Ho SY, Seo JW, Brown NA, Cook AC, Fagg NL, Anderson RH. Morphology of the sinus node in human and mouse hearts with isomerism of the atrial appendages. Br Heart J 1995;74:437–442. [PubMed: 7488461]
29. Cohen MS, Anderson RH, Cohen MI, Atz AM, Fogel M, Gruber PJ, Lopez L, Rome JJ, Weinberg PM. Controversies, genetics, diagnostic assessment, and outcomes relating to the heterotaxy syndrome. Cardiol Young 2007;17:29–43. [PubMed: 18039397]
30. Blaschke RJ, Hahurij ND, Kuijper S, Just S, Wisse LJ, Deissler K, Maxelon T, Anastassiadis K, Spitzer J, Hardt SE, Scholer H, Feitsma H, Rottbauer W, Blum M, Meijlink F, Rappold G, Gittenberger-de Groot AC. Targeted mutation reveals essential functions of the homeodomain transcription factor Shox2 in sinoatrial and pacemaking development. Circulation 2007;115:1830–1838. [PubMed: 17372176]
31. Berul CI, Aronovitz MJ, Wang PJ, Mendelsohn ME. In vivo cardiac electrophysiology studies in the mouse. Circulation 1996;94:2641–2648. [PubMed: 8921812]
32. Bae EJ, Noh CI, Choi JY, Yun YS, Kim WH, Lee JR, Kim YJ. Twin AV node and induced supraventricular tachycardia in Fontan palliation patients. Pacing Clin Electrophysiol 2005;28:126–134. [PubMed: 15679642]
33. Gurjarpadhye A, Hewett KW, Justus C, Wen X, Stadt H, Kirby ML, Sedmera D, Gourdie RG. Cardiac neural crest ablation inhibits compaction and electrical function of conduction system bundles. Am J Physiol Heart Circ Physiol 2007;292:H1291–H1300. [PubMed: 17172273]
34. Bharati S, Lev M. The course of the conduction system in single ventricle with inverted (L-) loop and inverted (L-) transposition. Circulation 1975;51:723–730. [PubMed: 1116258]
35. Meno C, Shimono A, Saijoh Y, Yashiro K, Mochida K, Ohishi S, Noji S, Kondoh H, Hamada H. lefty-1 is required for left-right determination as a regulator of lefty-2 and nodal. Cell 1998;94:287–297. [PubMed: 9708731]
36. Tessari A, Pietrobon M, Notte A, Cifelli G, Gage PJ, Schneider MD, Lembo G, Campione M. Myocardial Pitx2 differentially regulates the left atrial identity and ventricular asymmetric remodeling programs. Circ Res 2008;102:813–822. [PubMed: 18292603]

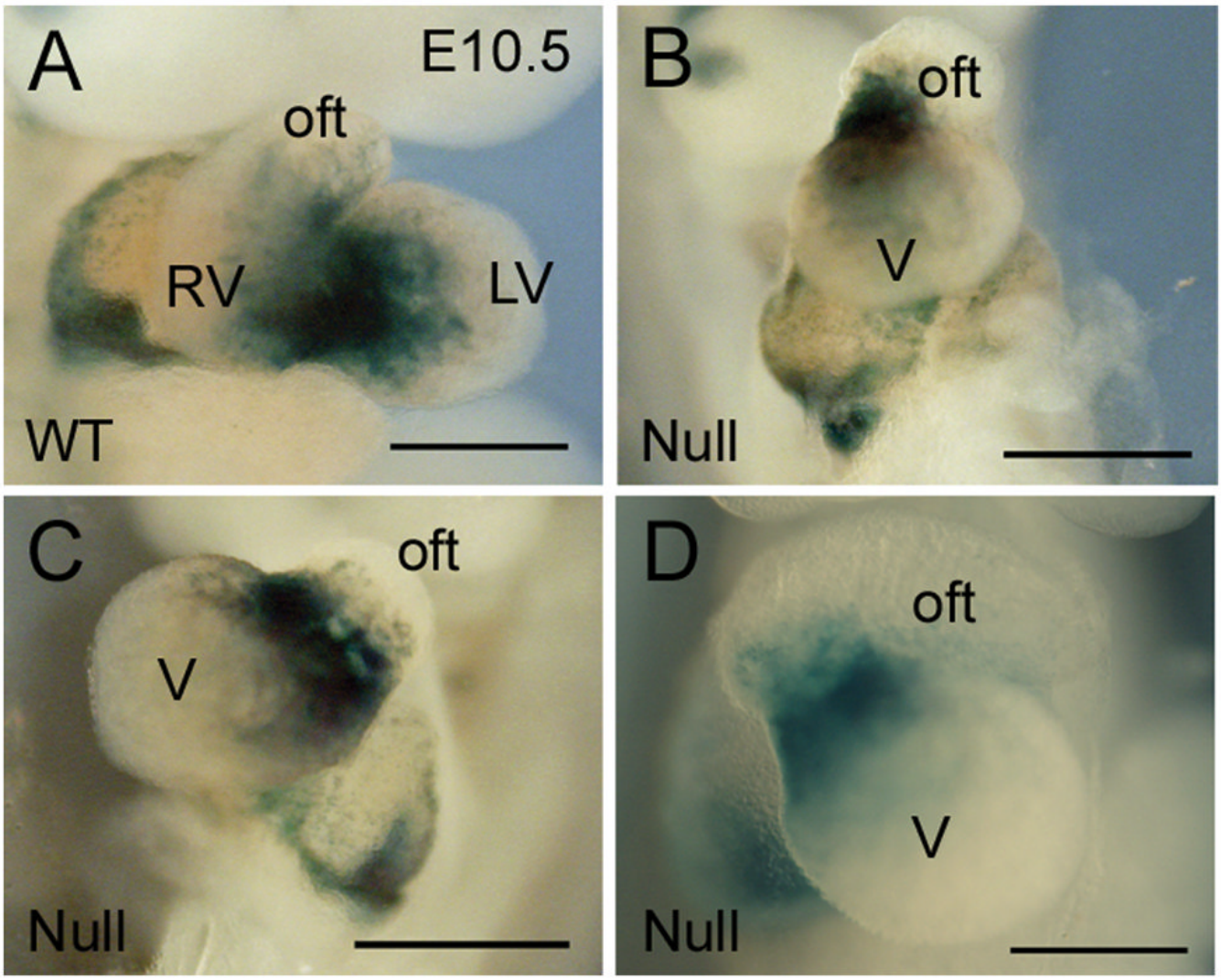


**Figure 1.**

Abnormal cardiac development in Zic3 embryos. A. Wild type embryo at e10.5 with typical d-looped ventricular configuration. B. Zic3 null embryo with d-looping and primitive ventricular configuration. C. Univentricular morphology with l-looping. The outflow tract arises from the leftward aspect of the ventricular chamber. There is dextrocardia with a rightward ventricular apex. D. Univentricular morphology with d-looping. The outflow tract arises from the rightward aspect of the ventricular chamber and the ventricular apex is directed leftward. X-gal staining illustrates the developing CCS. Scale bars are 300 μm. oft, outflow tract; LV, left ventricle; RV, right ventricle; V, ventricle.

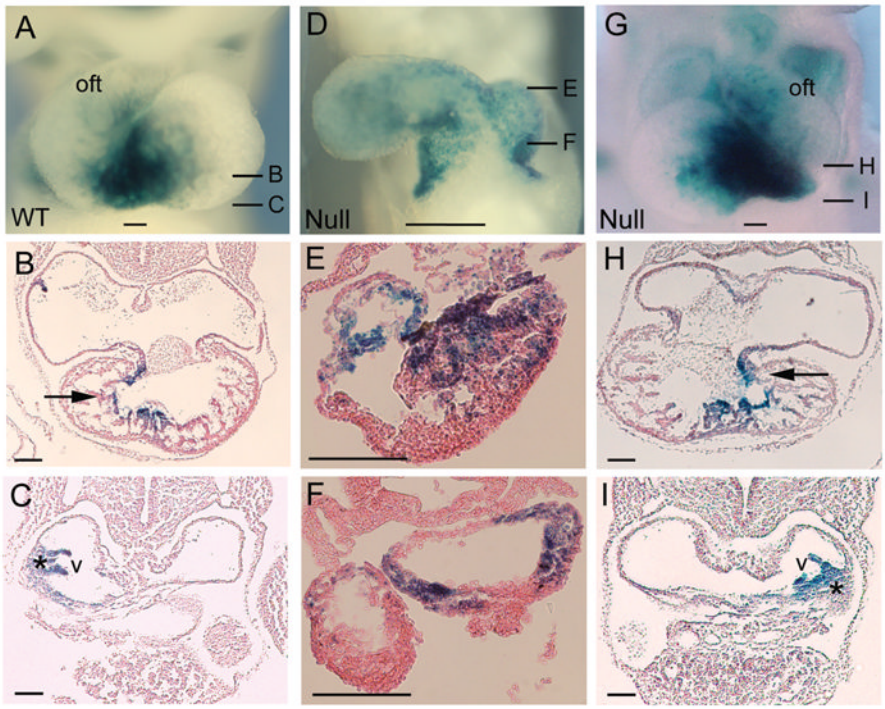


**Figure 2.**

Abnormal cardiac conduction system development in structurally abnormal embryos. Wild type (A-C) and Zic3 null (D-I) cardiac morphology and conduction system staining at e10.5. A. Wild type cardiac morphology with typical d-looping. B-C. Transverse sections at the levels indicated in (A) demonstrate the distal conduction system is a single linear band positioned rightward within the RV (arrow), and a normal SA nodal staining pattern restricted to the right atrium (*). D. Severe cardiac structural abnormalities with univentricular morphology and abnormal bilateralization of atrial staining. E-F. Sections at the levels indicated in (D) demonstrate abnormal atrial and ventricular development with conduction system staining in both the left and right aspects of the common atrium. G. Mirror image dextrocardia with l-looped ventricular morphology. H- I. Mirror image SA nodal patterning (*) with restriction of staining in the left atrium. The AV node and His bundle are leftward (arrow). Scale bars in A, D, G are 100 μm. Scale bars in B, C, E, F, H, I are 50 μm. Oft, outflow track; v, atrial venous valve.

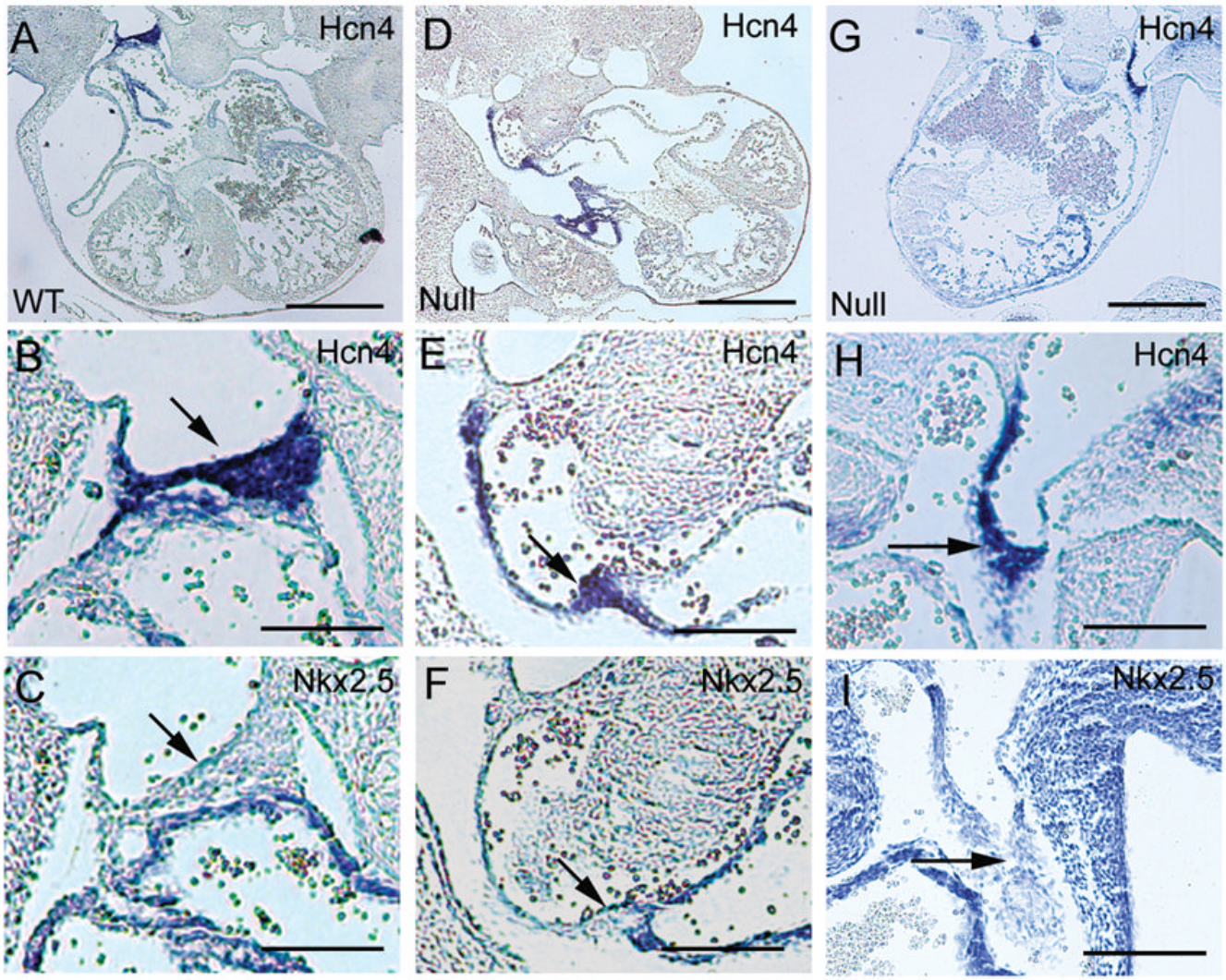


**Figure 3.**

SA node patterning is abnormal in e11.5 Zic3 null embryos. A-C. Molecular characterization in a wild type embryo. In (A) *Hcn4* expression delineates the SA node, positioned above the right atrium. B. High power view of SA node visualized in (A), demonstrating *Hcn4* staining of a wedge shaped area of tissue. *Nkx2.5* is excluded from this region (arrow) but is expressed in the surrounding myocardium in (C). D-F. Zic3 null embryo with abnormal anterior-posterior positioning of the ventricles and misalignment of the atria. The abnormally elongated SA node region is indicated by presence of *Hcn4* staining (D, E, arrow) and lack of Nkx2.5 staining (F). G-I. Zic3 null embryo with dextrocardia and common ventricle. Strong bilateral *Hcn4* staining was observed above the atria (G, H), and *Nkx2.5* staining was absent (I). Scale bars in A, D, G are 0.5 mm. Scale bars in B, C, E, F, H, I are 100 μm.

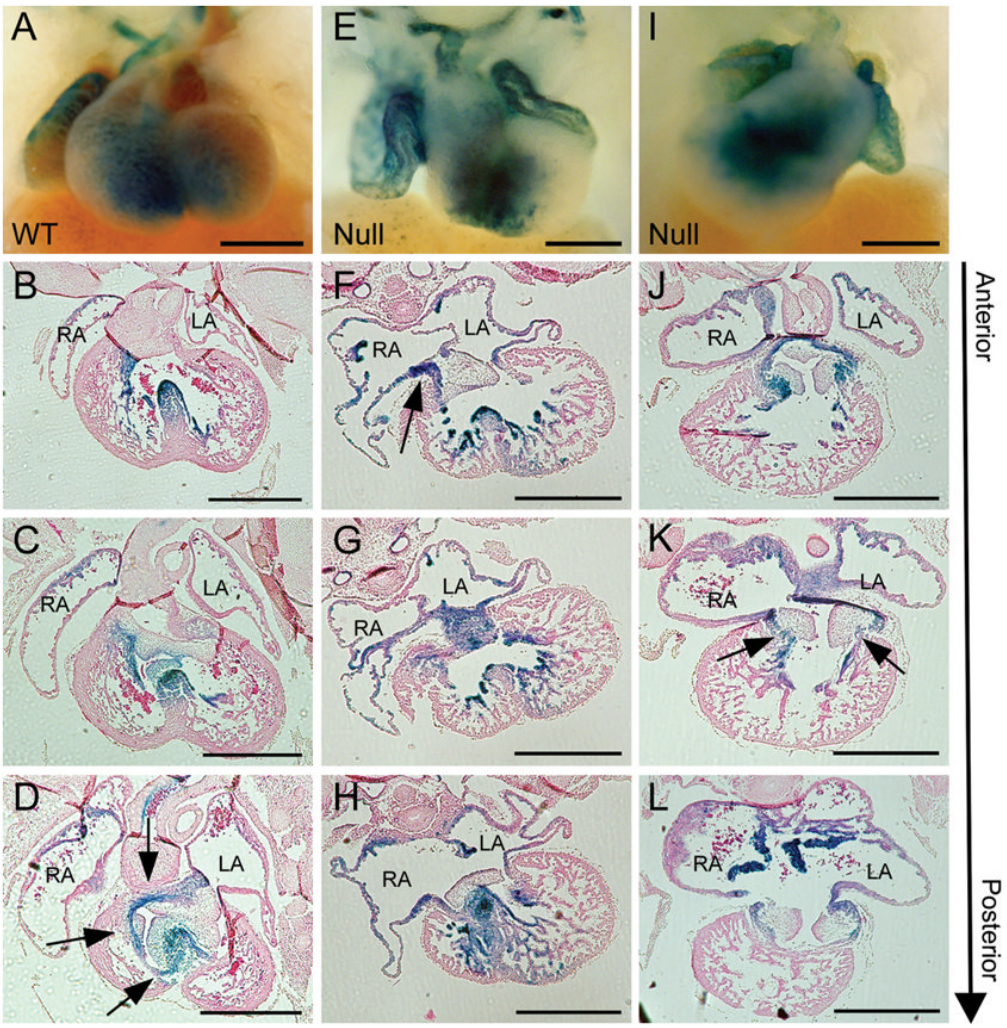


**Figure 4.**

Distal conduction system patterning is abnormal in Zic3 null embryos at e12.5. A-D. Normal patterning with a single staining band (arrows) from the crest of the developing interventricular septum to the AV node. E-H. Zic3 null embryo with accessory pathway connection (arrow) separate from the normal tract connecting the bundle branches and AV node. This tract resides lateral to the normal linear band connecting the right ventricular myocardium with the right aspect of the AV valve and right atrium. I-L. Zic3 null embryo with abnormal AV valve septation and positioning relative to the ventricular chambers with retention of the common AV valve and loss of normal septation between the mitral and tricuspid valves. The embryo has a primitive circumferential AV canal staining pattern giving rise to two separate tracts (arrows) from the developing AV node to the ventricular myocardium. Scale bars are 500 μm. RA, right atrium; LA, left atrium.

**Table 1**

Correlation of Structural and CCS Patterning Abnormalities

| Stage | Litters | Zic3 null embryos | Zic3 null structural abnormality | Zic3 null CCS abnormality | Embryos sectioned |
|---|---|---|---|---|---|
| e10.5 | 4 | 19 | 10 | 10 | 7 |
| e11.5 | 2 | 7 | 2 | 2 | 2 |
| e12.5 | 9 | 40 | 11 | 11 | 9 |
| e14.5 | 3 | 3 | 0 | 0 | 0 |
| e16.5 | 4 | 4 | 0 | 0 | 2 |

**Table 2**

Representative Cardiac Abnormalities in Zic3 Null Embryos

| Stage | Cardiac Structural Abnormalities | Conduction System Abnormalities |
|---|---|---|
| e10.5 | L-looped ventricles<br>Conotruncal malposition<br>Inferiorly displaced atria | Normal SA nodal patterning<br>Abnormal distal CCS patterning |
| e10.5 | L-looped ventricles<br>Widened conotruncus | SA node inversion |
| e10.5 | L-looped ventricles | Absent SA node<br>Abnormal distal CCS patterning |
| e10.5 | Univentricular morphology | Normal SA node patterning<br>Abnormal distal CCS patterning |
| e11.5 | Univentricular morphology<br>Bilateral superior vena cava | SA node duplication |
| e12.5 | DORV | Bi-atrial SA nodes<br>Duplication of AV nodal tissue<br>Accessory pathway connection |
| e12.5 | DILV | Bi-atrial SA nodes |
| e12.5 | Situs Inversus | Mirror image CCS elements |
| e12.5 | Univentricular morphology | Abnormal SA node patterning<br>Abnormal distal CCS patterning |

*CCS:* central conduction system. *DORV:* double outlet right ventricle. *DILV:* double inlet left ventricle.